
MULTI-OBJECTIVE OPTIMIZATION VIA EVOLUTIONARY ALGORITHM (MOVEA) FOR HIGH-DEFINITION TRANSCRANIAL ELECTRICAL STIMULATION OF THE HUMAN BRAIN *

Mo Wang¹, Kexin Lou^{1,2}, Zeming Liu¹, Pengfei Wei³, Quanying Liu¹

¹ Shenzhen Key Laboratory of Smart Healthcare Engineering,
Guangdong Provincial Key Laboratory of Advanced Biomaterials,
Department of Biomedical Engineering, Southern University of Science and Technology
² School of Information Technology and Electrical Engineering, University of Queensland
³ Shenzhen Institute of Advanced Technology, Chinese Academy of Sciences

Corresponding to Q.L. with liuqy@sustech.edu.cn

ABSTRACT

Transcranial temporal interference stimulation (tTIS) has been reported to be effective in stimulating deep brain structures in experimental studies. However, a computational framework for optimizing the tTIS strategy and simulating the impact of tTIS on the brain is still lacking, as previous methods rely on predefined parameters and hardly adapt to additional constraints. Here, we propose a general framework, namely multi-objective optimization via evolutionary algorithm (MOVEA), to solve the nonconvex optimization problem for various stimulation techniques, including tTIS and transcranial alternating current stimulation (tACS). By optimizing the electrode montage in a two-stage structure, MOVEA can be compatible with additional constraints (*e.g.* the number of electrodes, and additional avoidance regions), and MOVEA can accelerate to obtain the Pareto fronts. These Pareto fronts consist of a set of optimal solutions under different requirements, suggesting a trade-off relationship between conflicting objectives, such as intensity and focality. Based on MOVEA, we make comprehensive comparisons between tACS and tTIS in terms of intensity, focality and maneuverability for targets of different depths. Our results show that although the tTIS can only obtain a relatively low maximum achievable electric field strength, for example, the maximum intensity of motor area under tTIS is $0.42V/m$, while $0.51V/m$ under tACS, it helps improve the focality by reducing 60% activated volume outside the target. We further perform Analysis of Variance on the stimulation results of eight subjects with tACS and tTIS. Despite the individual differences in head models, our results suggest that tACS has a greater intensity and tTIS has a higher focality. These findings provide guidance on the choice between tACS and tTIS and indicate a great potential in tTIS-based personalized neuromodulation. MOVEA can not only optimize non-invasive electrical stimulations according to specific needs but also pave the way for using tTIS and tACS to uncover the causal relationship among brain region, cognitive function and behaviors.

Keywords Transcranial electrical stimulation (tES) · Multi-objective optimization · Evolutionary algorithm · Transcranial temporal interference stimulation (tTIS) · Transcranial alternating current stimulation (tACS) · Personalized neuromodulation

1 Introduction

Transcranial electrical stimulation (tES) is a non-invasive neuromodulation technique that has great potential in clinical applications, such as stroke treatment [31] and motor function improvement [14]. By injecting current through electrode

**Citation:* Wang et al. Title. Pages... DOI:000000/11111.

pairs on the scalp surface, tES can modulate neural activities and avoid complications from intracranial stimulations. tES has many specific implementations, among which transcranial direct current stimulation (tDCS) and transcranial alternating current stimulation (tACS) are the most commonly used in neuromodulation. These tES methods stimulate the brain by injecting an electrical current from the scalp ranging from 1–2 mA , such as the direct current in tDCS or a low-frequency alternating current in tACS. Some studies have reported that tES can improve behavioural performance in cognitive tasks. For example, 10 Hz tACS over the prefrontal cortex can enhance phonological word decision making [34], and 18 Hz tACS over right parietal lobe can significantly improve the visual processing [1]. However, due to the current diffusion effect, the current injected from the scalp by these traditional tES methods may not effectively penetrate the skull and generate focal stimulation in the deep brain region [10].

In order to improve the stimulation focality and depth of tES, efforts have been made from mainly two perspectives: new stimulation electrode configuration and new electrical stimulation technology. For the former, Bortoletto et al. have proposed high-density transcranial electrical stimulation (HD-tES) [2]. By replacing large sponge electrodes with a set of small saline electrodes, the high-density electrode configuration in HD-tES helps generate a more convergent electrical potential field. For the latter, Grossman and his colleagues have proposed a new stimulus strategy, namely transcranial temporal interfering stimulation (tTIS). tTIS applies two electrode pairs to introduce two high-frequency carriers with a small frequency difference, resulting in a low-frequency envelope at the target by coupling the carriers [16]. For example, two pairs of electrodes with 2000 Hz and 2010 Hz transcranial electrical stimulations can create a 10 Hz envelope at the specific target region. Due to nerves being less sensitive to high-frequency stimulation (*e.g.* 1 KHz) [22], the high-frequency carriers used for modulation avoid stimulation of tissues outside the target region. This effect will help limit effective stimulation to the low-frequency envelope zone, creating a more focal stimulation in tTIS. With these advances in tES, there have been several successful applications in tES-based brain modulation, such as memory consolidation [32], learning enhancement [47] and brain diseases treatment [23, 33]. However, there are cases where the same neuromodulation strategy produces different outcomes on a group of people, demonstrating inter-subject variability [38]. This inter-subject variability should be considered rather than neglected when designing personalized stimulation strategies. Therefore, computational models are needed to guide personalized tES stimulation strategy, to clarify how the inter-subject variability affects the performance of the stimulation strategy, and to improve the effectiveness of tES.

Various methods have been proposed for optimizing electrical stimulation strategy in tACS and tDCS [4, 21]. Unfortunately, those methods can not be directly applied to tTIS optimization, owing to the non-linearity and non-convex nature of the tTIS optimization problem. Some recent progress have been put forward to solve this non-convex problem [19, 29, 37, 43]. For instance, the exhaustive search algorithm to optimize the montages with the placement of activated electrodes and the corresponding injection current [29, 37]. The exhaustive search algorithm traverses all possible solutions and obtains the unique best solution based on the electrical field across the whole brain. Huang et al. [19] present a mathematical formulation of the optimization for tTIS with two arrays involving dozens of electrodes. Stoupis et al. [43] design an objective function as the ratio between the target region and other regions, obtaining the optimal montage with maximum objective value through a genetic algorithm. However, these methods have limitations, such as weak generalizability and high computational costs, which essentially limit their application in tTIS optimization. In particular, the algorithm from [19] is only suitable for a specific type of electrode arrays and cannot be applied to a general tTIS device. The genetic algorithm in [43] is sensitive to hyperparameters, and it can only optimize with the target ratio rather than direct control of the stimulation intensity. Moreover, in real tES practices, it is usual to consider some special avoidance areas, such as the eloquent area [25]. None of these optimization methods can set avoidance areas in designing optimization objectives. Thus, a general computational framework to optimize tES policy with multiple objectives (*e.g.* intensity, focality, and avoidance area) and constraints (*e.g.* safety protocol and electrode configuration) is highly needed for designing a personalized stimulation strategy.

To optimize tES strategies with multiple objectives, we introduce the concept of a constrained multi-objective optimization problem (CMOP) and the evolutionary algorithm for solving CMOP. These multi-objective optimization problems are usually non-convex problems for their discontinuity of objective functions. Moreover, the potential conflicts between these objectives in the CMOP make it difficult for traditional algorithms to obtain a globally optimal solution. Therefore, the trade-offs between some competing objectives in CMOP generate the Pareto front, which is a set of optimal solutions. Evolutionary algorithms are a well-known effective tool for solving these multi-objective problems [11]. Evolutionary algorithms can combine with Pareto relations, eliminate inferior solutions iteratively, and obtain optimal solutions. These solutions can be projected onto Pareto fronts, allowing for explicit visual comparisons of optimal solutions. This combination has been widely used in resource allocation problems, such as energy-efficient shop scheduling [9] and task offloading in edge computation [3]. To the best of our knowledge, evolutionary algorithms have not been used to solve CMOP for personalized tTIS optimization. How to define the objective functions in CMOP and how to empower evolutionary algorithms with appropriate optimizing search rules for tES optimization are worthy of further investigation.

In this work, we present a multi-objective optimization via evolutionary algorithm (MOVEA) for searching optimal tES policy. The MOVEA algorithm provides a general framework to solve CMOP for various tES stimulation methods, including tDCS, tACS and tTIS, allowing for posing multiple objectives in individual stimulation optimization. The major contributions of this work are summarized as follows.

- MOVEA defines an appropriate optimizing search rule and provides comprehensive comparisons of tACS and tTIS across multiple brain regions and stimulation objectives (Study 1 & Study 2).
- MOVEA is flexible for the additional design of constraints, such as safety constraints and avoidance areas (Study 3).
- MOVEA demonstrates how the inter-subject variability affects the tACS and tTIS performance (Study 4).

2 Method

In this section, we present a customized framework for multi-objective optimization of tES (Fig. 1). Our method requires individual structural MRI, HD-tES sensor montage and target areas as inputs. First, we pre-process these inputs: segmenting brain volume into tissues with different conductivity, co-registering individual structural MRI with HD-tES sensors, and defining target areas based on Brodmann atlas [28]. Then based on these pre-processed data, we can construct an accurate finite element method (FEM) head model and calculate the leadfield matrix for the selected ROI. This leadfield matrix is further utilized in the multi-objective optimization via evolutionary algorithm (MOVEA) for tES optimization. The detailed pipeline of MOVEA is illustrated in Fig. 1D. MOVEA provides a Pareto front that contains a set of optimal montages with trade-offs between conflicting objectives and the whole brain electrical distributions caused by these montages.

2.1 Construction of realistic head model

The head volume conductor model is also called the forward model or leadfield matrix in tES community which contains the mapping relationship between tES stimulation over the scalp and the induced electrical field in the brain. Many methods have been proposed to construct a realistic head model (*e.g.* boundary element method, finite element method, FEM). Here we use FEM for its accuracy and computation efficiency [40]. We calculate the leadfield matrix based on individual structural MRI and HD-tES sensor montage. Specifically, we first segment the head tissues from individual T1-weighted and T2-weighted MR images and then create the FEM head model by *Headreco* toolbox [35]. Our head model focuses on simulating the effects of extrinsic electrical stimulation. Since the electrical signals within the brain do not need to be considered in this problem, the model can be simplified to have no sources or sinks, where the Laplace equation (Eq. (1)) can be used to calculate the distribution V in the volume [15].

$$\nabla \cdot (\sigma \nabla V) = 0, \quad (1)$$

where σ is the conductivity of tissue which is assumed to be isotropic. The conductivity of tissues are assigned to $0.126 S/m$ (white matter), $0.276 S/m$ (gray matter), $1.65 S/m$ (cerebrospinal fluid (CSF)), $0.01 S/m$ (skull), $0.465 S/m$ (scalp), $0.5 S/m$ (eye), $2.5 e^{-14} S/m$ (air cavities), $1.0 S/m$ (saline), according to previous literatures [36, 39, 46].

Then, we put $n = 75$ electrodes on the FEM model's scalp at the corresponding position by SimNIBS 3.2 [41]. We choose the international 10/10 electrode placement system as the sensor montage and Cz as the reference electrode. Candidate electrodes are $1 \times 1 cm$ round saline electrodes with $4mm$ thickness. By sequentially applying unit current through each candidate electrode, we can obtain the electric field intensity for grey matter and white matter according to Eq. (1).

2.2 Multi-objective optimization via evolutionary algorithm (MOVEA)

We consider this mission to be a CMOP and its definition with M objective functions is as follows (2). In this study, the commonly use objective functions are *intensity* and *focality*, which refers to the averaged electric field strength across finite elements within ROI and the whole brain, respectively. The goal is to achieve maximum intensity and minimum focal length, subjecting to safety constraints, as shown in Eq. (2).

$$\begin{aligned} \min / \max \quad & f_m(x), m = 1, 2, \dots, M \\ \text{s.t.} \quad & \text{safety constraints,} \end{aligned} \quad (2)$$

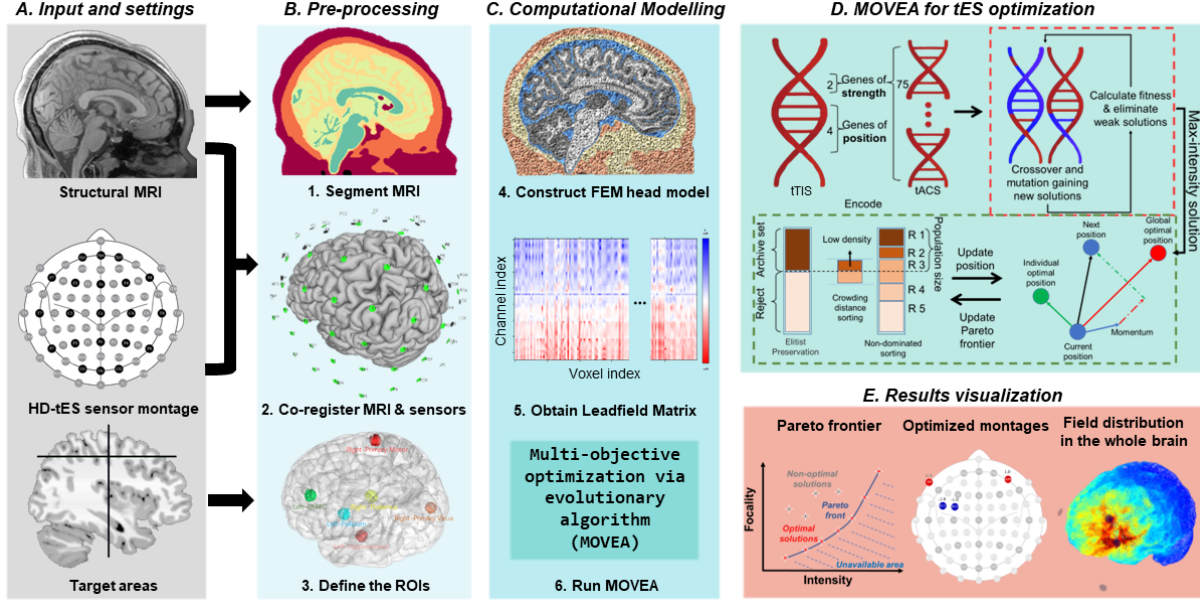


Figure 1: The framework of MOVEA for tES optimization. (A) *Input and setting*, consisting of individual T1-weighted or T2-weighted MR images (top), the HD-tES sensor montage (middle), and the selected target area or avoiding area (bottom). (B) *Pre-processing*, to segment the structural MRI (step 1), to co-register the brain with HD-tES sensors for aligning electrodes to the target space (step 2), and then define the ROIs by a sphere with a radius of 10 mm centred at the target area (step 3). (C) *Computational modelling*, to construct a realistic head model using the finite element method based on Laplace's equation and electrical conductivity of each brain tissue (step 4), to obtain the leadfield matrix (LFM), which contains information on the distribution of electric fields in each voxel when a current is injected by each electrode (step 5), to run MOVEA with LFM and ROIs as input (step 6). (D) *Pipeline of MOVEA for tES optimization*. First, the activated channels and the corresponding current intensities are encoded to sites on the gene. Second, the solution for the electric field intensity at the target ROI is calculated by crossover and mutation (Red box), which is then set as the initial value for the multi-objective optimization problem. For multi-objective optimization, in the decision space, the next position of each solution is determined by its own velocity, its historical optimal position, and the globally optimal solution (Right of the green box). In the objective space, the dominant solution set is obtained by non-dominated sorting, crowding distance sorting, and elitist preservation (Left of the green box). After several iterations, the Pareto front is obtained. (E) *Results visualization*, to illustrate and quantify the results of MOVEA, which includes the Pareto front for target intensity versus focality (left), the optimized tES policy (*i.e.* locations of tES electrodes & injected currents, middle), the whole-brain field distribution induced by tES (right).

where x denotes the index of the activation electrode and the corresponding current intensity, and $f_m(x)$ represents the m -th objective function ($m \in \{1, 2, \dots, M\}$). We will introduce the MOVEA algorithm to solve this CMOP problem in subsequent subsections.

2.2.1 Simulating the tACS-induced electric field in the brain

Considering the input current s by tACS electrodes, the induced electric field in the brain can be computed with the leadfield matrix A as $E = As$, where E denotes the triaxial electric field intensity. According to [42], the averaged electric field intensity across a brain area Ω in the field direction, E_Ω , can be formulated as Eq. (3).

$$E_\Omega = \frac{1}{G_\Omega} \int_\Omega \|E\| dG = \frac{1}{G_\Omega} \int_\Omega \sqrt{E_x^2 + E_y^2 + E_z^2} dG, \quad (3)$$

where G_Ω denotes the total volume in the brain area Ω , and x , y and z represent three orthogonal directions.

2.2.2 Simulating the TI-induced electric field in the brain

The electric field in the brain generated by transcranial temporal interference stimulation with two pairs of tTIS electrodes can be calculated according to Grossman et al. [16], as Eq. (4):

$$\left| \vec{E}_{AM}(\vec{r}) \right| = \begin{cases} 2 \left| \vec{E}_2(\vec{r}) \right| & |\vec{E}_1(\vec{r})| < |\vec{E}_2(\vec{r})| \cos(\alpha) \\ 2 \left| \vec{E}_2(\vec{r}) \times (\vec{E}_1(\vec{r}) - \vec{E}_2(\vec{r})) \right| / \left| \vec{E}_1(\vec{r}) - \vec{E}_2(\vec{r}) \right| & \text{otherwise} \end{cases} \quad (4)$$

where $E(\vec{r})$ are the electric field at location r coming from one pair electrodes and α is the angle between \vec{E}_1 and \vec{E}_2 . The Eq. (4) holds only when $\alpha < 90^\circ$ and $|\vec{E}_1(\vec{r})| > |\vec{E}_2(\vec{r})|$, or the sign of \vec{E}_2 and the numbering of the channels should be inverted and swapped respectively.

2.2.3 Designing the safety constraints

There are some additional constraints to ensure the safety of human participants. The total injection current and the maximum individual injection current are denoted as I_{tot} and I_{ind} , respectively. For m electrodes, considering the presence of a reference electrode and according to Kirchhoff's current law, Eq. (5) constrains that the sum of the absolute values of the current intensity of candidates and reference electrode should be smaller than $2 * I_{tot}$. The constraints, Eq. (6) and Eq. (7) are set to avoid skin irritation, discomfort, and heating at the individual electrode interface.

$$g_1(s) = \sum_m |s_m| + \left| \sum_m s_m \right| \leq 2I_{tot}, \quad (5)$$

$$g_2(s) = |s_m| \leq I_{ind}, \quad (6)$$

$$g_3(s) = \left| \sum_m s_m \right| \leq I_{ind}, \quad (7)$$

To quantify the degree of violation to constraints [48], we define a constraint violation (CV) index in Eq.(8). Since the constraint Eq.(6) is guaranteed during the encoding (Fig.1D), CV is a summation of the normalized violations to the constraint Eq. (5 & 7).

$$CV = \max\left(\frac{\left| \sum_m s_m \right| - I_{ind}}{I_{ind}}, 0\right) + \max\left(\frac{\sum_m |s_m| + \left| \sum_m s_m \right| - 2I_{tot}}{2I_{tot}}, 0\right), \quad (8)$$

where the function $\max(x, 0)$ outputs the maximal value between x and 0.

2.2.4 Formulating CMOP for optimizing tES policy

We formulate a CMOP problem for optimizing tES policy. The goal of the optimization is to achieve the strongest electric field *intensity* in the target region with the highest *focality* (*i.e.* the smallest whole-brain electric field intensity). A solution of the stimulation strategy includes the position of stimulation electrodes in the standard 10-10 system and the injected current in each electrode.

Since the intensity and the focality often fail to achieve optimal values simultaneously, the result of the multi-objective optimization problem is a *Pareto front*. The Pareto front comprises optimum solutions across several objective functions (*e.g.* intensity and focality). The performance of these solutions on a specified objective function cannot be further enhanced without degrading the performance of other objective functions. We say the solution s_a *Pareto dominates* the solution s_b if the solution s_a does not perform worse than the solution s_b on any objective function and the solution s_a performs better than the solution s_b on some objective functions. Thus, the Pareto front contains all solutions that are not Pareto dominated by others.

In the case of considering constraint violations, the Pareto front is more complicated since the constraints in the multi-objective optimization problem may be satisfied or violated. We say the individual a Pareto dominates the individual b if one of the following conditions are met:

- Individual a satisfies the constraint, but individual b violates it;

- Both the individual a and b meet the constraint conditions, and individual a Pareto dominates individual b in all other indicators;
- Both the individual a and individual b are not satisfied, but the constraint violation of individual a is smaller.

2.2.5 Solving CMOP via evolutionary algorithm

Due to the nonlinearity and non-convex nature of the tES model, applying multi-objective algorithms such as *NSGAII* [7] to solve this problem directly is time-consuming. Moreover, *NSGAII* hardly finds the optimal electrode montages converging to the strongest electric field intensity. In this study, we employ the evolutionary algorithm to solve the CMOP.

We present a combination of genetic algorithms and particle swarm algorithms (Fig. 1D). Specifically, we use a single-objective genetic algorithm to find the maximum intensity target and then apply it as prior knowledge to search the Pareto front using multiple objective particle swarm optimization (MOPSO) [8]. As a heuristic algorithm, MOPSO keeps the previously discovered non-dominated particles as the optimal global solutions, and then other particles use them to guide their evolution.

In MOVEA, we first encode the montages to make them readable by a model. For tACS, we use an array with a length of n , each point representing the injected current strength of the corresponding channel. For tTIS, we use an array with a length of 6. The first two represent the strength of each pair of electrodes, and the last four represent the position of the selected channel.

Then, we use a genetic algorithm for the one-objective search. We assume that when the electric field strength is at its highest, the injected current is pooled on the channel with the greatest impact on the target, so we limit the current intensity to 1 or -1 *mA*. Since the genetic algorithm is biologically inspired, we treat the encoded array as a gene and get a new phenotype after performing operations such as mutation and crossover [17]. Then, we compare the new results with the old results and weed out the poor performers. Through some iterations, we obtain the solution for maximum intensity.

Finally, we perform multi-objective optimizations to obtain the Pareto front of trade-off targets. The multi-objective particle swarm algorithm treats a solution as a particle, and the array's values are treated as the coordinates of each dimension in high-dimensional decision space. Moreover, we release the limitation by the assumption mentioned before so that the particles can search the Pareto front more flexibly. With prior knowledge, particle evolution is influenced by themselves and the elite solution. Particles calculate the position of the next moment according to their optimal historical position and the optimal global position of all the particles. After obtaining the new position, we calculate the performance of particles corresponding to the current position and decide whether to update their optimal position. For each iteration, we choose the better of the Pareto relationships, and if they do not Pareto dominate each other, we choose the solutions those particles located in less populated areas in objective space by crowding distance sorting [8].

3 Experiments and Results

3.1 Dataset and experimental setup

In this work, we use the T1 and T2 MRI data from the HCP S1200 Release dataset [44] to build the head model. Optimization and visualization methods are implemented by Python 3.8 and run with NVIDIA V100. The population size and epoch of stage one are set to 100 and 100. The population size, archive set size, mesh size and epoch of stage two are set to 100, 100, 10, and 100. The other settings can be found in the codes. All statistical analyses for the electric field distribution of brain voxels are conducted with *Origin* (Version 2022. OriginLab Corporation, Northampton, MA, USA).

3.2 Study 1: Optimization of tTIS and tACS for six target regions.

To compare the effects of optimized tTIS and tACS, we perform MOVEA on the same head model to achieve Pareto fronts for different brain regions. We select six target regions, including three in the superficial areas (*i.e.* motor cortex, DLPFC and V1) and three in the deep brain areas (*i.e.* hippocampus, pallidum and thalamus), which have been widely targeted in previous tES studies [6, 18, 19, 43].

Here are some basic settings for this experiment. We define the target region as a 10 *mm* sphere at the target point. The target point is selected based on the Brodmann atlas, and the value is fine-tuned to highlight the difference between depth and depth. The MOVEA algorithm aims to maximize the electric field intensity inside the target region while minimizing the average electric field across the brain. The orientation of the electric field is free. According to safety

protocols [13], we add two safety constraints on currents for both tTIS and tACS: i) the sum of current intensity across all electrodes should be no larger than 2mA (*i.e.* $I_{tot} \leq 2mA$), and ii) the absolute value of the current at each individual electrode should be no larger than 1mA (*i.e.* $I_{ind} \leq 1mA$).

We run the intensity optimization experiment based on the above settings, and the results of an example subject (HCP sub877168) are shown here. Fig. 2 illustrates 12 Pareto fronts for each of the 6 target ROIs, including three brain areas in the superficial layer (*i.e.* motor cortex, DLPFC, and V1) and three in the deep brain (*i.e.* hippocampus, pallidum, and thalamus).

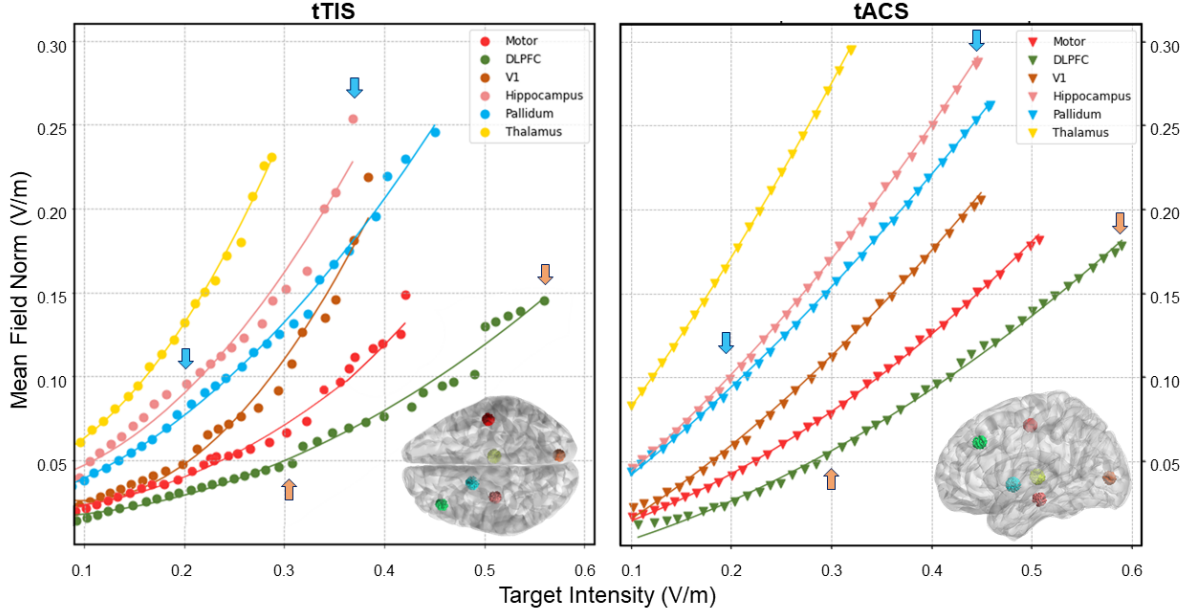


Figure 2: The Pareto fronts obtained by MOVEA for tTIS (left) and tACS (right). We set the target area in the motor cortex, DLPFC, V1, hippocampus, pallidum and thalamus. The ROIs with 10 mm radius are shown in the axial and sagittal view. MOVEA optimizes the tES policy for each ROI separately, which generates the Pareto fronts for target intensity versus mean field norm (*i.e.* focality). The Pareto fronts are obtained by using the realistic FEM head model from a specific subject (*i.e.* HCP sub877168). As examples, we visualize the arrow-marked tTIS and tACS policies in Fig. 3. *MNI coordinates*: DLPFC, [-39, 34, 37]; motor, [47, -13, 52]; V1, [14, -99, -3]; hippocampus, [-31, -20, -14]; pallidum, [-17, 3, -1]; thalamus, [10, -19, 6].

The Pareto front reveals a trade-off between intensity and focality. Both the selection of the targeted region and the stimulation modality impact the results. Specifically, the depth of the thalamus is 62 mm. The maximum intensity of it under tTIS is 0.28V/m, while 0.33V/m under tACS. When we select a superficial target motor, the maximum intensity under two stimulations improves to 0.42V/m and 0.51V/m, respectively. The Pareto front comprises solutions that are optimum across target intensities. Each point in the Pareto front represents an optimal stimulation strategy. For example, Fig. 3 visualizes the four solutions indicated by arrows in Fig. 2. The visualization shows the results for a target area in DLPFC (Fig. 3A,C,E,G) and hippocampus (Fig. 3B,D,F,H). Fig. 2 demonstrates the location of activation electrodes, their injected current and the induced electric fields in the brain. For safety reasons, the injected current intensity of each electrode in tES follows the pre-defined constraint (*i.e.* total injected current: 2mA for tTIS and tACS).

The solution that achieves maximum electrical field intensity at the target region is refereed as *Max intensity*, and the solution that achieves maximal focality at the target region while satisfying the intensity constrain (*i.e.* 0.3V/m for DLPFC, 0.2V/m for hippocampus) is refereed as *Specific intensity*. We compare the results for *Max intensity* and *Specific intensity* in Fig. 3, and find that tTIS and tACS induce electric fields in large brain areas in both conditions. These solutions induce electrical fields at areas outside of the target ROIs, resulting in a leakage problem. This leakage problem will aggravate when the target electric field intensity increases. When the target ROI is in a superficial brain region, this leakage problem can be mitigated and the induced electric field is more likely to be focal.

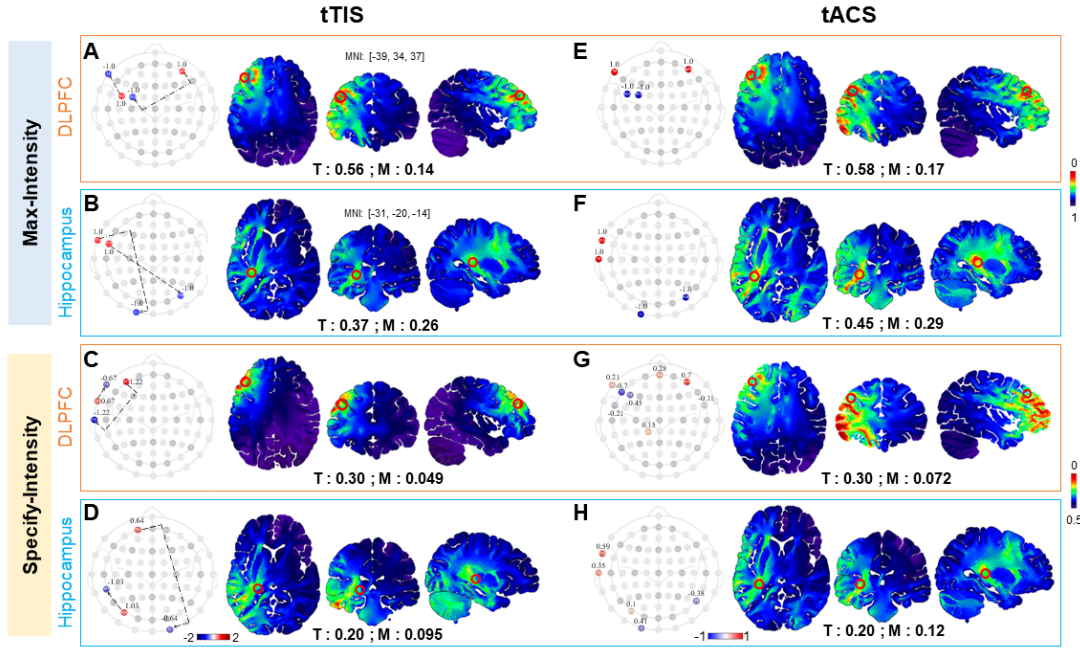


Figure 3: The optimized tES policy by MOVEA for tTIS (A-D) and tACS (E-H). We present the results for a target area in the **DLPFC** (A, C, E, G) and **hippocampus** (B, D, F, H), respectively. These results correspond to the specific solutions in the Pareto front marked in Fig. 2. **Max-Intensity** refers to an objective function to maximize the intensity of the electric field (T in V/m unit) in the target area regardless of the focality (M in V/m unit), while **Specify-Intensity** refers to an objective function to maximize the focality of the electric field in target area given a fixed electric field intensity T (i.e. $T = 0.3$ for DLPFC, $T = 0.2$ for hippocampus). In each panel, we illustrate the pairs of activation electrodes and their injected current (left), the three views (i.e. axial, coronal, and sagittal view) of the induced electric fields in the brain (right), where the red circle indicates the target area. The injected current intensity of each electrode in tES obeys a pre-defined constraint in MOVEA for safety reasons (i.e. total injected current: $2mA$ for tTIS and tACS). *Abbr:* tES, transcranial electrical stimulation; tTIS, transcranial temporal interference stimulation; tACS, transcranial alternating current stimulation; DLPFC, dorsolateral prefrontal cortex; T , the averaged electric field within the ROI; M , the averaged electric field across the whole brain.

To compare the focality of the electric fields generated by tTIS and tACS, we run MOVEA with the desired target intensity $0.25V/m$ and calculate the proportions of voxels with intensity greater than different levels of threshold (i.e. $0.10V/m$, $0.20V/m$, and $0.25V/m$) (Table. 1). The results show that tTIS can generate more focal electric fields in all six target regions compared to that caused by tACS. In particular, as the threshold increases from $0.10v/m$ to $0.25v/m$, the thresholded volume ratio Vol of DLPFC drops from 6.31% to 0.38% (Table. 1). The reduced proportion Δ greatly reduces from 59.81% to 30.33%. Compared to other target regions, the reduced proportions gradually increase when the stimulation threshold increases. Furthermore, the volume ratio for tACS in region V1 is larger than in the deeper region Pallidum, showing a more dispersed electric field. There is also a greater improvement from tTIS stimulation, with the reduced proportion Δ increasing from 61.33% to 82.86%.

3.3 Study 2: Optimized tES policy across the whole brain

To evaluate the achievable intensity induced by two stimulations across the whole brain, we conduct experiments at two types of target regions: 1) a group of voxels; 2) a single voxel. In the first experiment, these groups of voxels are defined as voxels in the 10 mm spheres at the center of each Brodmann region. By setting each of these spheres as targets, we optimize maximal intensity with 2 mA for both tTIS and tACS. According to Fig. 4A, the maximum intensity achieved by both stimulations decreases as the depth of the target increases. As we only define the stimulation target as the center sphere in each Brodmann region, some other voxels might be omitted from this setting. To further investigate how is the achievable intensity distributed across the brain, we set the target regions as randomly selected single voxels in the second experiment. For computational efficiency, we sampled 20000 voxels from 1467981 voxels of gray matter and white matter. The result of achievable intensity for targeting at a single voxel level is shown in Fig. 4B. Under this

Table 1: The proportion of voxels greater than the corresponding threshold when the intensity of target is $2.5V/m$. The head model used in MOVEA is built on HCP sub877168. Vol represents the proportion of the whole brain above the threshold. The smaller the Vol, the better the focality. Δ refers to the proportion of reduced activated voxels compared to Vol_{tACS} .

Target	MNI coordinate	Depth (mm)	Threshold (V/m)	Vol (%)		Δ (%)
				tACS	tTIS	
DLPFC	[-39, 34, 37]	7	0.10	15.7	6.31	59.81
			0.20	1.89	0.80	57.7
			0.25	0.54	0.38	30.33
Motor	[47, -13, 52]	10	0.10	26.9	10.7	60.22
			0.20	4.32	1.48	65.74
			0.25	1.51	0.49	67.15
V1	[14, -99, -3]	20	0.10	69.3	26.8	61.33
			0.20	17.7	3.46	80.45
			0.25	8.40	1.44	82.86
Pallidum	[-17, 3, -1]	45	0.10	62.6	42.0	32.91
			0.20	16.5	6.50	60.30
			0.25	6.50	2.29	64.77
Hippocampus	[-31, -20, -14]	40	0.10	79.8	65.0	18.55
			0.20	21.6	11.0	49.07
			0.25	8.59	3.27	61.93
Thalamus	[10, -19, 6]	62	0.10	99.5	95.5	4.02
			0.20	61.5	33.4	45.69
			0.25	30.3	14.8	51.16

setting, tACS still achieves higher induced intensity. Moreover, the maximum intensity distribution induced by tACS is uneven, with more significant intensity at superficial regions, whereas tTIS induces a more evenly distributed pattern (Fig.6B). The maximum intensity regions induced by these two methods are similar(Fig.6B).

3.4 Study 3: Optimal tES design to avoid activating a specific brain region

To verify the performance of MOVEA to avoid activating a specific brain region (*i.e.* avoidance zone), we design an optimization experiment with the avoidance region in a superficial area of right DLPFC (dorsal) (MNI: [42,37,31]) and the target region in the deep area of it (MNI: [42,24,24]). We obtain the optimal stimulation policy for the following four stimulation setups:

1. The tACS setup optimized by SimNIBS, consisting of two conventional electrodes attached on $5cm \times 5cm$ patches, each of which can inject a maximum of $2mA$ current;
2. The HD-tACS setup optimized by SimNIBS, consisting of two pairs of electrodes in 10-10 standard (more details in Sec. 2.1);
3. The HD-tACS setup optimized by MOVEA, consisting of two pairs of electrodes in 10-10 standard (more details in Sec. 2.1);
4. The tTIS setup optimized by MOVEA, consisting of two pairs of electrodes in 10-10 standard (more details in Sec. 2.1).

The results are visualized in Fig.5. Specifically, the traditional tACS causes the weakest stimulation in the target region ($T = 0.09$ in Fig.5 A). When both are using HD-tACS setup (Fig.5 B-C), MOVEA can significantly reduce the electric

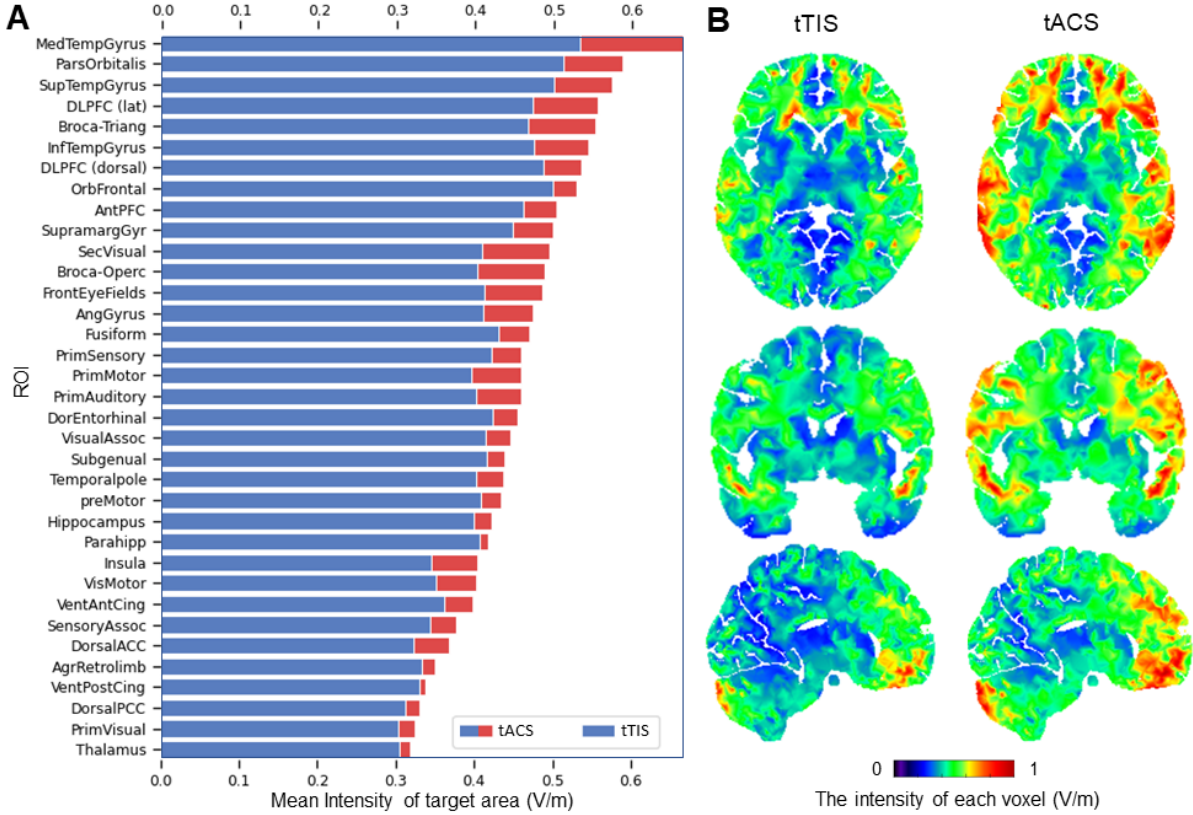


Figure 4: The maximal intensity achieved by MOVEA in each brain region with $2mA$ of tES on the scalp. (A) The maximal mean intensity achieved in the 35 brain regions. The Brodmann atlas defines the regions. In all 35 brain regions, the current intensity that tACS can achieve is higher than tTIS, and the increment of tACS over tTIS is indicated with the red box. (B) The spatial distribution of the maximal intensity achieved by tTIS (left) and tACS (right).

field intensity in the avoidance zone ($A = 0.23$), compared with SimNIBS ($A = 0.29$). Considering both the target region and avoidance zone, we find tTIS achieves the best manipulation ($T = 0.30$, $A = 0.23$, in Fig.5 D).

3.5 Study 4: Inter-subject variability

Individual head models have a high degree of inter-subject variability for the differences in head shape and spatial tissue distribution. To investigate how the variability of the individual head model impacts the optimization of tES policy, we select eight subjects from the HCP dataset [44] and build individual head models based on their T1 and T2 images.

In this study, we choose DLPFC and hippocampus as the representative of shallow targets and deep targets, respectively. The Pareto fronts for intensity and focality of these two targets are obtained by MOVEA. As shown in Fig. 6, the head of each subject is segmented differently for their head shape and tissue spatial distribution. These differences in tissue segmentation lead to variability in head models, resulting in different Pareto fronts for each subject. For example, when targeting at DLPFC, the maximum achievable intensity induced by tTIS varies from $0.45V/m$ to $0.65V/m$.

Further, we measure the distribution of the electric field at each voxel when the target ROI obtains the maximum intensity. In Fig. 7, we can find that when targeting at the shallow target DLPFC (Fig. 7A), the difference in the electric field intensity between the target region (blue) and the whole brain (red) is bigger. Moreover, we do the two-way analysis of variance for eight subjects under the same simulation's way or target, observing the influence of another factor and the individual differences, as well as their interactions, on the experimental. The statistical results validate statistically significant effects of simulation mode ($P < 0.001$), individual differences ($P < 0.001$), and simulation mode \times individual differences ($P < 0.001$). Similar results are found between the simulation target selection and individual differences ($P_s < 0.001$).

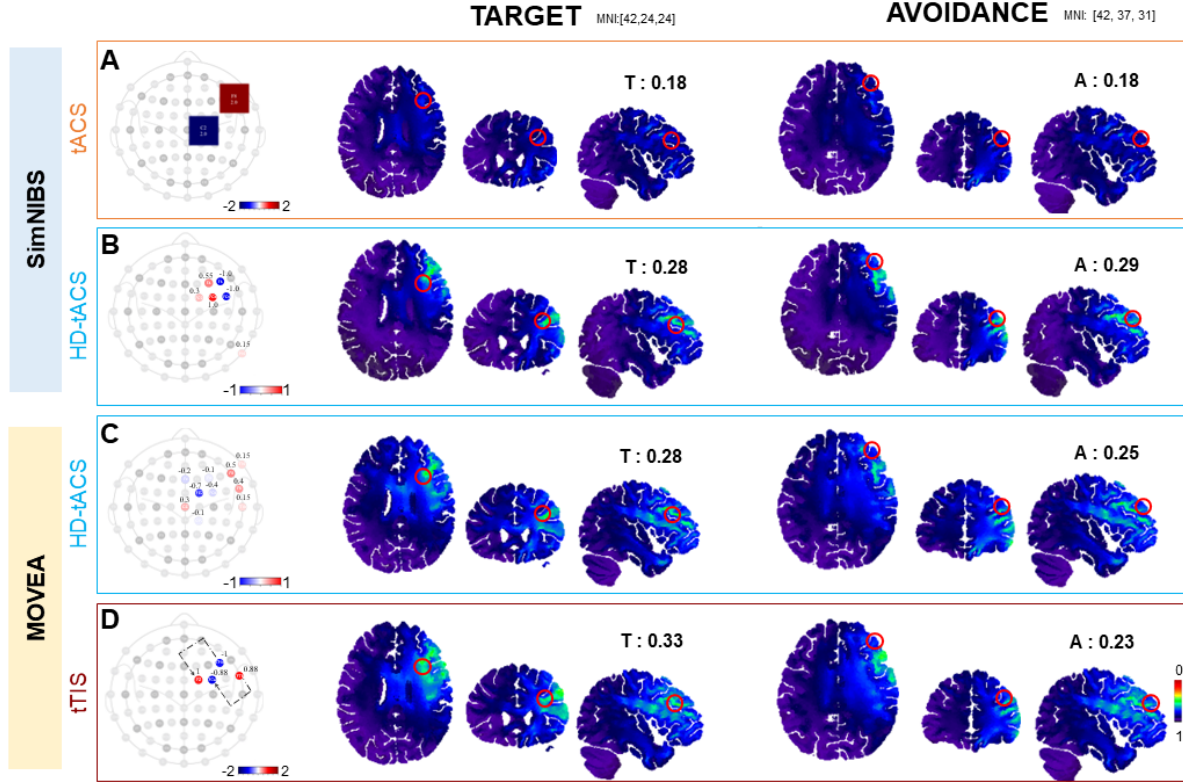


Figure 5: Optimization results with avoidance zones. Four stimulation strategies were used. (A) The conventional electrodes consist of two $5\text{cm} \times 5\text{cm}$ patches, each of which can inject a maximum of 2mA current; (B) HD-tACS optimized by SimNIBS; (C) HD-tACS optimized by MOVEA; (D) tTIS optimized by MOVEA. The first column of each row represents the electrode distribution, the second column is the visualization of the electric field distribution in the target ROI, and the third column is the visualization of the electric field distribution in the avoidance region. *Abbr.*: tACS, transcranial alternating current stimulation; HD-tACS, high-defined transcranial alternating current stimulation; tTIS, transcranial temporal interference stimulation; T , the averaged electric field within the target ROI; A , the averaged electric field within the avoidance zone.

4 Discussion

In this paper, we present an evolutionary algorithm-based model MOVEA for solving multi-objective optimization in transcranial electrical stimulation. Without pre-defined stimulation parameters, MOVEA provides a computational framework for optimizing the tES stimulation strategy with multiple constraints, obtaining optimal solutions as Pareto fronts. MOVEA can further assist the comparison and selection of individual stimulation strategies, showing great potential in the application of personalized tES.

Accelerating genetic algorithm with a two-stage structure: The tES optimization can be formulated as a CMOP problem [49]. Directly solving this CMOP problem using a genetic algorithm, such as NSGA2 [12], is time-consuming and easy to fail due to the ample search space. In this study, we equip MOVEA with a two-stage structure to accelerate optimization and obtain a complete Pareto front through constraint relaxation. In the first stage, MOVEA finds the optimal solution in a limited space according to reasonable assumptions. In the second stage, MOVEA constructs a complete Pareto front under the guidance of the previous solution. This two-stage structure can vastly improve efficiency. Compared with using the multi-objective genetic algorithm NSGA2 directly, our method can shorten the optimization time from 8 hours to about 1 hour (see computer settings in Sec. 3.1). Moreover, MOVEA can find the maximum intensity solution. For example, when we try to stimulate the Motor area under tACS, the maximum intensity achieved by MOVEA is 0.51V/m , while 0.35V/m by NSGA2 [24].

Comparison of stimulation intensity between tTIS and tACS: Based on the Pareto fronts obtained by MOVEA, we compared the performance of tACS and tTIS in terms of stimulation intensity. Regarding maximum intensity achieved

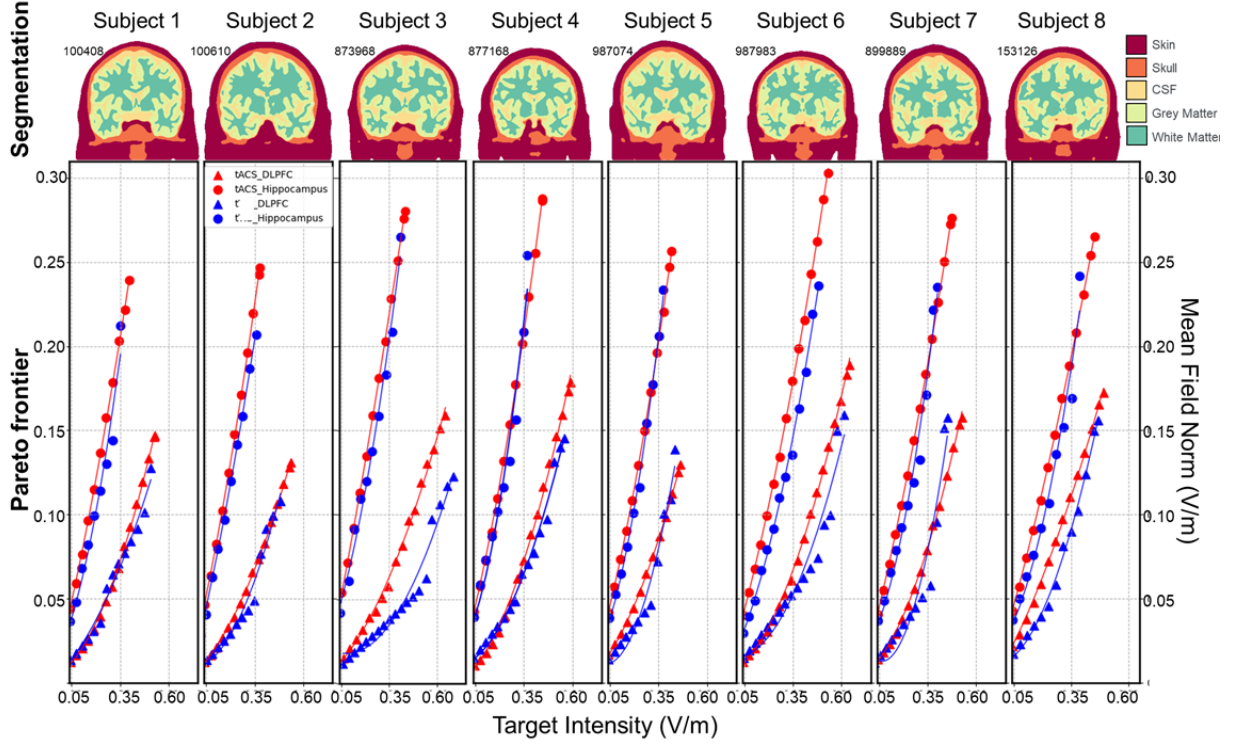


Figure 6: Sensitivity to the individualized head model. The results are from 8 subjects in HCP dataset, showing inter-subject variability. (Up) Segmented tissues from individual T1 MRI, including skin, skull, CSF, grey matter, and white matter. The number shows the index of the HCP subject. (Bottom) Pareto front optimized with the target area in the DLPFC (triangles) or in the hippocampus (circles). The results of tTIS and tACS are indicated in red and blue, respectively. Each point in the Pareto fronts is an optimal tES strategy with a specific target intensity.

by tES, despite the differences in head models, we get consistent results with the research by exhaustive search (*e.g.* free field for the Motor area under TIs: $0.56V/m$, tACS: $0.60V/m$) [37]. It is worth noting that Rampersad et al. choose a large target area and counted the largest electric fields in it, while we choose a smaller area and counted the average electric fields as the target to realize precise stimulation. Moreover, our results showed that tACS yields higher induced current intensity compared to tTIS (Fig. 2&4&6). This finding is consistent with previous literature [20, 37]. Our tTIS simulations were based on the method proposed by Grossman et al. [16], shown in Eq. 9.

$$|\vec{E}(\vec{r})| = ||\vec{E}_1(\vec{r}) + \vec{E}_2(\vec{r})| - |\vec{E}_1(\vec{r}) - \vec{E}_2(\vec{r})||, \quad (9)$$

But when the stimulation method is the conventional tACS, only the first term, $||\vec{E}_1(\vec{r}) + \vec{E}_2(\vec{r})||$, should be used. Moreover, the second term, $-||\vec{E}_1(\vec{r}) - \vec{E}_2(\vec{r})||$, is always negative, combined with the similarity of TIs and tACS montage at maximum intensity, which might explain why the maximum intensity of tTIS is smaller than that of tACS.

Focality and steerability of tTIS: We examined the focality and steerability of tTIS. Fig. 2 suggests that the focality of tTIS is better than that of tACS at the same target intensity. As Table 1 shows, tTIS induces less activation outside the target region under the same conditions as tACS. This phenomenon may be explained by the stimulation mechanism of tTIS, as only the low-frequency electrical signals obtained by coupling two high-frequency electrical inputs can genuinely affect neural activity. A similar finding is also shown in Fig.3, where tTIS generate weak stimulations outside of the target region (*e.g.* DLPFC and hippocampus). At the same time, tACS requires more electrodes to achieve the same target max-focality. Our findings suggest that tTIS has higher adaptability even when the number of electrodes is limited. In addition, when targeting the superficial region (*e.g.* V1) via tACS, the activation ratio Vol is greater than that of a deeper region (*e.g.* Pallidum). The large activation ratio might be attributed to the V1's proximity to the CSF. As [20] suggests, CSF is highly conducting media, and the closer the target is to the CSF, the more diffused the electric field is. On the contrary, tTIS can well manipulate the activation ratio Vol in deeper regions. According to Table 1, when targeting at V1, tTIS has a lower Vol compared to tACS, resulting in a highly reduced ratio in Δ , suggesting that tTIS can improve the focality. In addition, the results of MOVEA with an avoidance zone suggest that

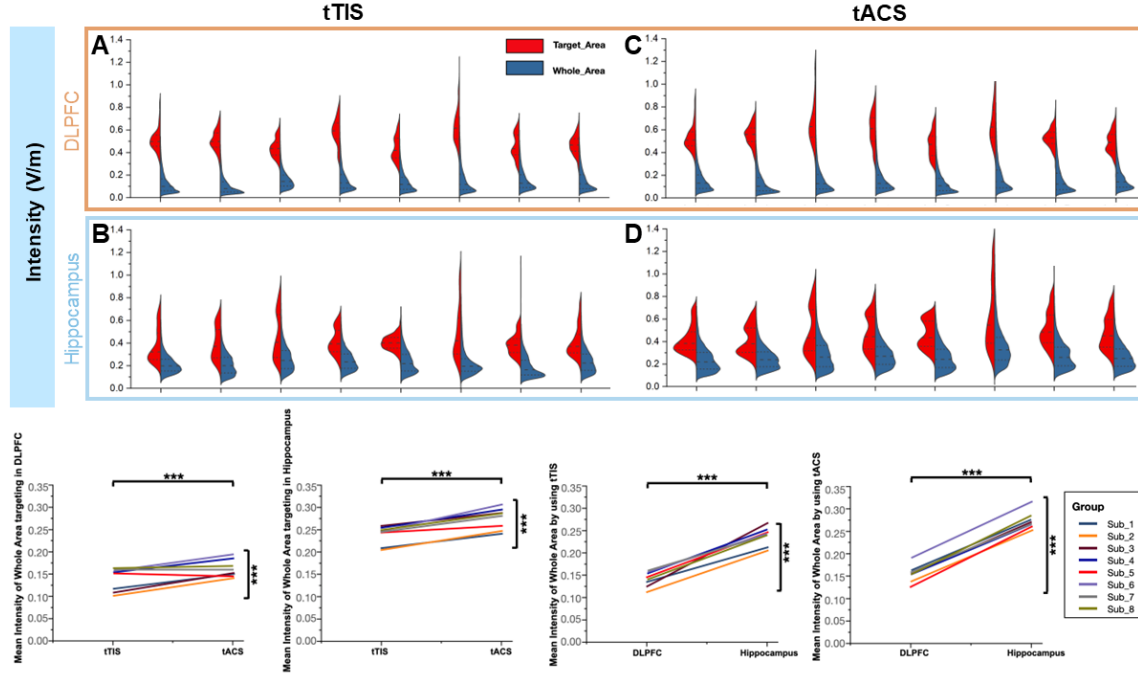


Figure 7: Statistical analysis of electric field strength distribution in eight subjects. We calculated the proportion of voxels at each electric field strength for the corresponding target area (red-half-violin) and whole brain (blue-half-violins) separately. The split violin chart shows the results with DLPFC (A, C) and hippocampus (B, D) as the target region under tTIS (A, B) and tACS (C, D). To explore the overall effect of stimulation mode and target selection (tTIS vs tACS, DLPFC vs Hippocampus) on subjects, we compared the mean field intensity of the whole-brain region after stimulation, and conducted a two-way analysis of variance combined with individual differences between groups (E). *** represents $p < 0.001$.

tTIS is more operable. Fig. 5 shows the stimulation intensity of tDCS, HD-tACS and tTIS, where tTIS outperforms other stimulation methods. Traditional tACS, which uses large electrode patches in stimulation, has failed to generate satisfactory electric fields in the brain (Fig. 5A). This focality problem can be improved with smaller electrodes, as suggested by [27]. Therefore, the performances of HD-tACS optimized by SimNIBS and MOVEA are better than traditional tACS (Fig. 5B&C). Moreover, because of the characteristics of tTIS, the activation of shallow areas can be mitigated but not entirely avoided when the electric field converges at the target. This property further improves the convergence and steerability, which is in line with previous study [6, 20]. Altogether, despite its relatively low intensity, we can benefit from the high focality and steerability of tTIS.

Advantages of MOVEA compared to SimNIBS: SimNIBS implements the avoidance region by weighting the terms corresponding to the matrix. During the convex optimization iterative solution, the smaller weight has a limited intensity reduction across the avoidance region, and the larger weight will seriously impact the optimization of the target area. While MOVEA uses the Pareto relationship to solve this problem, providing trade-offs to select feasible solutions. SimNIBS is not available for tTIS optimization because it only designs the solution algorithm for tACS. We add the encoding and the electric field expression function of tTIS to the algorithm, providing a more comprehensive framework for tES.

Inter-subject variability: We test MOVEA with head models from eight subjects. The difference of inter-subject variability shown by Pareto fronts in Fig. 6 and electric field strength of voxels at the target or the whole brain under maximum intensity in Fig. 7. The results indicate that individuals need different stimulation strategies to achieve the maximum intensity at the target. This difference might come from individual anatomical structures, such as skull thickness, CSF layout, and cortical folding [26]. Our results are well consistent with previous literature [18, 29], suggesting that customized tTIS is necessary to enhance the neuromodulation efficacy. At the same time, the results of two-way analysis of variance showed that there are significant differences in target selection, individual differences and their interactions ($P_s < 0.001$), the same as simulation modes and individual differences. These statistical results indicate the effectiveness of our target area and stimulus selection, and reveal the new function between the two factors

above and individual differences. Moreover, despite the inter-subject variability, tTIS and tACS effects are reliable, and the overall trend well fits previous studies.

Limitations and future directions: While MOVEA can provide a set of optimal solutions for flexible and personalized tES, limitations in this study are worth mentioning. First, MOVEA is time-consuming, although it is already much faster than the traditional CMOP solver. The most time-consuming step in MOVEA is calculating the electric field of millions of voxels distributed across the brain. It takes about one hour for each subject. The time cost would limit its applications in closed-loop neuromodulation. One of our future directions is to further improve the efficiency by designing new metrics or optimization algorithms. For example, since the electric field distribution outside the target area is not necessarily taken into account, we can reduce model resolution inside the regions of interest to accelerate the algorithm. Second, our results demonstrate the merit of tTIS on focality and steerability, even if we only use two pairs of stimulation electrodes. According to previous literature, these advantages of tTIS can be further improved by using multiple pairs of electrodes [6, 30], or by using inter-sectional Short Pulse Stimulation [45]. In the future, these properties can be incorporated into MOVEA framework, promoting the personalized tES design with desired intensity and steerability. Lastly, building the individualized head models require their MRI images, which are not easy and economical to acquire. Some methods already exist to optimize tES without individual MRI, for example, using EEG signals to guide tES design [5]. By integrating those methods into MOVEA, the cost of tES optimization can be largely reduced, and tES-based clinical treatments would be more feasible in real-world applications.

5 Conclusion

In conclusion, we presented MOVEA for searching the optimal tES policy. MOVEA is a general framework for multiple stimulation methods (*e.g.* tDCS, tACS, and tTIS), compatible with additional constraints (*e.g.* the number of electrodes and the intensity in the avoidance region). It can obtain a set of solutions at each level of objective (*e.g.* different intensities), avoiding the situation that specific solutions cannot be obtained due to individual differences [18]. MOVEA can provide personalized tES strategies with customized constraints, offering a potential tool for clinical treatments and uncovering the causal relationship among brain area, cognitive function, and behavior.

Acknowledgments

This work was funded in part by the National Key R&D Program of China (2021YFF1200804), National Natural Science Foundation of China (62001205), Guangdong Natural Science Foundation Joint Fund (2019A1515111038), Shenzhen Science and Technology Innovation Committee (20200925155957004, KCXFZ2020122117340001), Shenzhen-Hong Kong-Macao Science and Technology Innovation Project (SGDX2020110309280100), Shenzhen Key Laboratory of Smart Healthcare Engineering (ZDSYS20200811144003009), Guangdong Provincial Key Laboratory of Advanced Biomaterials (2022B1212010003).

References

- [1] Luca Battaglini, Andrea Ghiani, Clara Casco, and Luca Ronconi. Parietal tacs at beta frequency improves vision in a crowding regime. *Neuroimage*, 208:116451, 2020.
- [2] Marta Bortoletto, Claudia Rodella, Ricardo Salvador, P. C. Miranda, and Carlo Miniussi. Reduced current spread by concentric electrodes in transcranial electrical stimulation (tes). *Brain Stimulation*, 9:525–528, 2016.
- [3] Arash Bozorgchenani, Farshad Mashhadi, Daniele Tarchi, and Sergio A. Salinas Monroy. Multi-objective computation sharing in energy and delay constrained mobile edge computing environments. *IEEE Transactions on Mobile Computing*, 20:2992–3005, 2021.
- [4] André Russowsky Brunoni and Marie-Anne Vanderhasselt. Working memory improvement with non-invasive brain stimulation of the dorsolateral prefrontal cortex: a systematic review and meta-analysis. *Brain and cognition*, 86:1–9, 2014.
- [5] Andrea Cancelli, Carlo Cottone, Franca Tecchio, Dennis Q Truong, Jacek Dmochowski, and Marom Bikson. A simple method for eeg guided transcranial electrical stimulation without models. *Journal of neural engineering*, 13(3):036022, 2016.
- [6] Jiaming Cao and Pulkrit Grover. Stimulus: Noninvasive dynamic patterns of neurostimulation using spatio-temporal interference. *IEEE Transactions on Biomedical Engineering*, 67(3):726–737, 2019.

- [7] Anuch Chaube, Lyés Benyoucef, and Manoj Kumar Tiwari. An adapted nsga-2 algorithm based dynamic process plan generation for a reconfigurable manufacturing system. *Journal of Intelligent Manufacturing*, 23(4):1141–1155, 2012.
- [8] CA Coello Coello and Maximino Salazar Lechuga. Mopso: A proposal for multiple objective particle swarm optimization. In *Proceedings of the 2002 Congress on Evolutionary Computation. CEC'02 (Cat. No. 02TH8600)*, volume 2, pages 1051–1056. IEEE, 2002.
- [9] Min Dai, Dunbing Tang, Adriana Giret, and Miguel A. Salido. Multi-objective optimization for energy-efficient flexible job shop scheduling problem with transportation constraints. *Robotics Comput. Integr. Manuf.*, 59:143–157, 2019.
- [10] Abhishek Datta, Varun Bansal, Julian Diaz, Jinal Patel, Davide Reato, and Marom Bikson. Gyri-precise head model of transcranial direct current stimulation: improved spatial focality using a ring electrode versus conventional rectangular pad. *Brain stimulation*, 2(4):201–207, 2009.
- [11] Kalyanmoy Deb. Multi-objective optimization using evolutionary algorithms. In *Wiley-Interscience series in systems and optimization*, 2001.
- [12] Kalyanmoy Deb, Samir Agrawal, Amrit Pratap, and Tanaka Meyarivan. A fast elitist non-dominated sorting genetic algorithm for multi-objective optimization: Nsga-ii. In *International conference on parallel problem solving from nature*, pages 849–858. Springer, 2000.
- [13] Jacek P Dmochowski, Abhishek Datta, Marom Bikson, Yuzhuo Su, and Lucas C Parra. Optimized multi-electrode stimulation increases focality and intensity at target. *Journal of neural engineering*, 8(4):046011, 2011.
- [14] Matteo Feurra, Giovanni Bianco, Emiliano Santarnecchi, Massimiliano Del Testa, Alessandro Rossi, and Simone Rossi. Frequency-dependent tuning of the human motor system induced by transcranial oscillatory potentials. *Journal of Neuroscience*, 31(34):12165–12170, 2011.
- [15] David Jeffrey Griffiths. College, r. *Introduction to electrodynamics*, 3, 1999.
- [16] Nir Grossman, David Bono, Nina Dedic, Suhasa B Kodandaramaiah, Andrii Rudenko, Ho-Jun Suk, Antonino M Cassara, Esra Neufeld, Niels Kuster, Li-Huei Tsai, et al. Noninvasive deep brain stimulation via temporally interfering electric fields. *cell*, 169(6):1029–1041, 2017.
- [17] Ahmad Hassanat, Khalid Almohammadi, Esra’a Alkafaween, Eman Abunawas, Awni Hammouri, and VB Surya Prasath. Choosing mutation and crossover ratios for genetic algorithms—a review with a new dynamic approach. *Information*, 10(12):390, 2019.
- [18] Yu Huang and Abhishek Datta. Comparison of optimized interferential stimulation using two pairs of electrodes and two arrays of electrodes. In *2021 43rd Annual International Conference of the IEEE Engineering in Medicine & Biology Society (EMBC)*, pages 4180–4183. IEEE, 2021.
- [19] Yu Huang, Abhishek Datta, and Lucas C Parra. Optimization of interferential stimulation of the human brain with electrode arrays. *Journal of neural engineering*, 17(3):036023, 2020.
- [20] Yu Huang and Lucas C Parra. Can transcranial electric stimulation with multiple electrodes reach deep targets? *Brain stimulation*, 12(1):30–40, 2019.
- [21] Yu Huang, Chris Thomas, Abhishek Datta, and Lucas C Parra. Optimized tdcS for targeting multiple brain regions: an integrated implementation. In *2018 40th Annual International Conference of the IEEE Engineering in Medicine and Biology Society (EMBC)*, pages 3545–3548. IEEE, 2018.
- [22] Bruce Hutcheon and Yosef Yarom. Resonance, oscillation and the intrinsic frequency preferences of neurons. *Trends in neurosciences*, 23(5):216–222, 2000.
- [23] Yasuto Inukai, Kei Saito, Ryoki Sasaki, Shota Tsuiki, Shota Miyaguchi, Sho Kojima, Mitsuhiro Masaki, Naofumi Otsuru, and Hideaki Onishi. Comparison of three non-invasive transcranial electrical stimulation methods for increasing cortical excitability. *Frontiers in Human Neuroscience*, 10, 2016.
- [24] et.al. Jazzbin. *geatpy: The genetic and evolutionary algorithm toolbox with high performance in python*, 2020.
- [25] Barbara C Jobst, Ritu Kapur, Gregory L Barkley, Carl W Bazil, Michel J Berg, Gregory K Bergey, Jane G Boggs, Sydney S Cash, Andrew J Cole, Michael S Duchowny, et al. Brain-responsive neurostimulation in patients with medically intractable seizures arising from eloquent and other neocortical areas. *Epilepsia*, 58(6):1005–1014, 2017.
- [26] Ilkka Laakso, Satoshi Tanaka, Soichiro Koyama, Valerio De Santis, and Akimasa Hirata. Inter-subject variability in electric fields of motor cortical tdcS. *Brain stimulation*, 8(5):906–913, 2015.

- [27] Ilkka Laakso, Satoshi Tanaka, Marko Mikkonen, Soichiro Koyama, and Akimasa Hirata. Variability in tdc electric fields: Effects of electrode size and configuration. In *2017 XXXIInd General Assembly and Scientific Symposium of the International Union of Radio Science (URSI GASS)*, pages 1–4, 2017.
- [28] C Lacadie, RK Fulbright, J Arora, R Constable, and X Papademetris. Brodmann areas defined in mni space using a new tracing tool in bioimage suite. In *Proceedings of the 14th annual meeting of the organization for human brain mapping*, volume 771, 2008.
- [29] Sangjun Lee, Chany Lee, Jimin Park, and Chang-Hwan Im. Individually customized transcranial temporal interference stimulation for focused modulation of deep brain structures: a simulation study with different head models. *Scientific reports*, 10(1):1–11, 2020.
- [30] Sangjun Lee, Jimin Park, Chany Lee, Chang-Hwan Im, et al. Multipair transcranial temporal interference stimulation for improved focalized stimulation of deep brain regions: A simulation study. *Computers in Biology and Medicine*, 143:105337, 2022.
- [31] Stephanie Lefebvre, Laurence Dricot, Patrice Laloux, Wojciech Gradkowski, Philippe Desfontaines, Frederic Evraud, Andre Peeters, Jacques Jamart, and Yves Vandermeeren. Neural substrates underlying stimulation-enhanced motor skill learning after stroke. *Brain*, 138(1):149–163, 2015.
- [32] Caroline Lustenberger, Michael R Boyle, Sankaraleengam Alagapan, Juliann M Mellin, Bradley V Vaughn, and Flavio Fröhlich. Feedback-controlled transcranial alternating current stimulation reveals a functional role of sleep spindles in motor memory consolidation. *Current Biology*, 26(16):2127–2136, 2016.
- [33] Marcus Meinzer, Robert Darkow, Robert Lindenberg, and Agnes Flöel. Electrical stimulation of the motor cortex enhances treatment outcome in post-stroke aphasia. *Brain : a journal of neurology*, 139 Pt 4:1152–63, 2016.
- [34] Vera Moliadze, Leon Sierau, Ekaterina Lyzhko, Tristan Stenner, Michael Werchowski, Michael Siniatchkin, and Gesa Hartwigsen. After-effects of 10 hz tacs over the prefrontal cortex on phonological word decisions. *Brain stimulation*, 12(6):1464–1474, 2019.
- [35] Jesper D Nielsen, Kristoffer H Madsen, Oula Puonti, Hartwig R Siebner, Christian Bauer, Camilla Gøbel Madsen, Guilherme B Saturnino, and Axel Thielscher. Automatic skull segmentation from mr images for realistic volume conductor models of the head: Assessment of the state-of-the-art. *Neuroimage*, 174:587–598, 2018.
- [36] Alexander Opitz, Walter Paulus, Susanne Will, Andre Antunes, and Axel Thielscher. Determinants of the electric field during transcranial direct current stimulation. *Neuroimage*, 109:140–150, 2015.
- [37] Sumientra Rampersad, Biel Roig-Solvas, Mathew Yarossi, Praveen P Kulkarni, Emiliano Santarnecchi, Alan D Dorval, and Dana H Brooks. Prospects for transcranial temporal interference stimulation in humans: a computational study. *NeuroImage*, 202:116124, 2019.
- [38] Fatemeh Sadeghihassanabadi, Jonas Misselhorn, Christian Gerloff, and Simone Zittel. Optimizing the montage for cerebellar transcranial alternating current stimulation (tacs): a combined computational and experimental study. *Journal of Neural Engineering*, 19(2):026060, 2022.
- [39] Guilherme B Saturnino, André Antunes, and Axel Thielscher. On the importance of electrode parameters for shaping electric field patterns generated by tdc. *Neuroimage*, 120:25–35, 2015.
- [40] Guilherme B Saturnino, Kristoffer H Madsen, and Axel Thielscher. Electric field simulations for transcranial brain stimulation using fem: an efficient implementation and error analysis. *Journal of neural engineering*, 16(6):066032, 2019.
- [41] Guilherme B Saturnino, Oula Puonti, Jesper D Nielsen, Daria Antonenko, Kristoffer H Madsen, and Axel Thielscher. Simnibs 2.1: a comprehensive pipeline for individualized electric field modelling for transcranial brain stimulation. *Brain and human body modeling*, pages 3–25, 2019.
- [42] Guilherme Bicalho Saturnino, Hartwig Roman Siebner, Axel Thielscher, and Kristoffer Hougaard Madsen. Accessibility of cortical regions to focal tes: Dependence on spatial position, safety, and practical constraints. *NeuroImage*, 203:116183, 2019.
- [43] Dimitrios Stoupis and Theodoros Samaras. Non-invasive stimulation with temporal interference: Optimization of the electric field deep in the brain with the use of a genetic algorithm. *bioRxiv*, 2022.
- [44] David C Van Essen, Stephen M Smith, Deanna M Barch, Timothy EJ Behrens, Essa Yacoub, Kamil Ugurbil, Wu-Minn HCP Consortium, et al. The wu-minn human connectome project: an overview. *Neuroimage*, 80:62–79, 2013.
- [45] Mihály Vöröslakos, Yuichi Takeuchi, Kitt Brinyiczki, Tamás Zombori, Azahara Oliva, Antonio Fernández-Ruiz, Gábor Kozák, Zsigmond Tamás Kincses, Béla Iványi, György Buzsáki, et al. Direct effects of transcranial electric stimulation on brain circuits in rats and humans. *Nature communications*, 9(1):1–17, 2018.

- [46] T.A. Wagner, M. Zahn, A.J. Grodzinsky, and A. Pascual-Leone. Three-dimensional head model simulation of transcranial magnetic stimulation. *IEEE Transactions on Biomedical Engineering*, 51(9):1586–1598, 2004.
- [47] Miles Wischniewski, Paul Zerr, and Dennis JLG Schutter. Effects of theta transcranial alternating current stimulation over the frontal cortex on reversal learning. *Brain stimulation*, 9(5):705–711, 2016.
- [48] Yonas Gebre Woldesenbet, Gary G Yen, and Biruk G Tessema. Constraint handling in multiobjective evolutionary optimization. *IEEE Transactions on Evolutionary Computation*, 13(3):514–525, 2009.
- [49] Shenghua Zhu, Minmin Wang, Mingwei Ma, Haonan Guan, and Shaomin Zhang. An optimization approach for transcranial direct current stimulation using nondominated sorting genetic algorithm ii. In *2021 43rd Annual International Conference of the IEEE Engineering in Medicine & Biology Society (EMBC)*, pages 4337–4340. IEEE, 2021.